

ORFIT dedicated thermo-plastic nets, supports and cushions. Images were reconstructed in six phases across the respiratory cycle with CT50 being the exhale image set used for MR image registration.

MRI was acquired with a body coil on a 1.5T SIEMENS Aera. The patients were set up with the same patients' immobilization and positioning devices as for CT imaging thanks to a MR compatible ORFIT table. Axial Single Shot Fast Spin Echo T2-weighted with fat suppression Spectral Adiabatic Inversion Recovery (SPAIR) and motion reduction method (BLADE) was first acquired with breath triggering on exhale. Then ultra-fast gradient echo T1-w with parallel acquisition and Dixon reconstruction techniques (VIBE DIXON) allowed the acquisition in exhale breath hold. Finally injected T1-w Fast Low Angle Shot (Turbo FLASH) imaging sequence was acquired with breath triggering on exhale.

Results: The lesion was not always visible on 4D CT scan, even on images with contrast enhancement hence the need of MRI to better define the lesion. Target motion range was assessed based on fiducials' displacement.

The use of the same table and immobilization device for MRI minimized uncertainties due to patient position for image registration.

T1-w VIBE DIXON sequence was useful to register MR sequences based on fiducials' position, as they were the most visible on this sequence. The two breath-triggered (expiration phase) sequences (T2 SPAIR BLADE and injected T1-w Turbo FLASH) provided a motion artifact free image necessary to accurately delineate the lesion.

An example of MR/CT50 registration and target volume definition is illustrated on Figure 1.

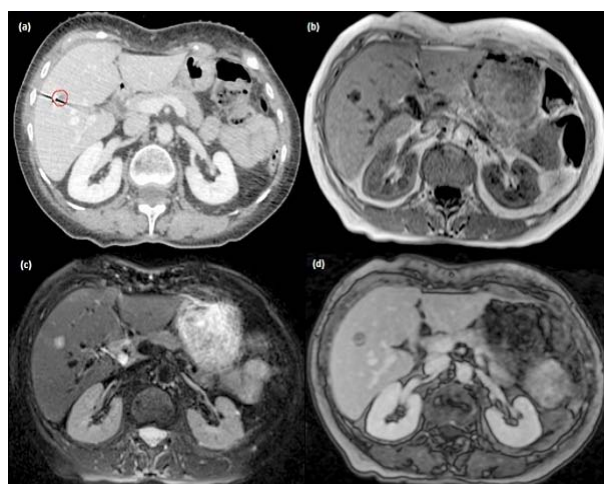


Figure 1: Example of registered image for a breast metastasis in liver segment V (a): injected CT50 with target contour delineated in red thanks to the MRI sequences. (b): T1 DIXON_w. (c):T2 SPAIR BLADE, (d): injected T1-w Turbo FLASH

Conclusion: The use of the same table and immobilization device for CT and MRI combined with the use of MR imaging sequences optimized to account not only for the dedicated table and immobilization devices but also for the gold seeds visualization and the tumor delineation allow high precision target delineation.

EP-1829

Evaluation of metal artifact reduction (MAR) algorithm for patients with a bilateral hip implant

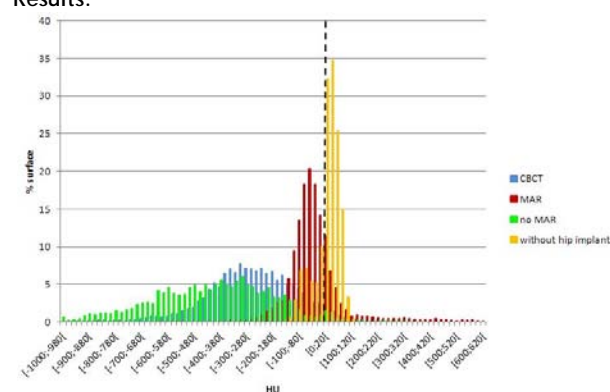
A. Morel¹, J. Molinier¹, L. Bedos¹, N. Aillères¹, D. Azria¹, P. Fenoglietto¹

¹ICM - Val d'Aurelle, Radiothérapie, Montpellier, France

Purpose or Objective: Analyze the information stemming from three methods of images acquisition for soft tissues between a bilateral hip implant.

Material and Methods: Six patients with a bilateral hip implant were selected for this study. For every patient, 3 series of images were compared. The two first ones were performed with GE Optima CT580 simulator, one by using the metal artifacts reduction (MAR) algorithm and the other one without. The third series was acquired by Cone Beam Computed Tomography (CBCT) during the first session of treatment. For every series, the same rectangular ROI was drawn on a frontal slice, in the soft tissues situated between the two prostheses. The average Hounsfield Units (HU) and the standard deviation (σ), corresponding to the noise in the image, were collected. According to the same methodology, the images of 12 patients without hip implant were studied in order to have a reference of the average Hounsfield Unit (HUref) in this anatomic region and to compare it with the obtained results for images of patients with a bilateral hip implant.

Results:



For the cohort of patients without hip implant, HUref was of $11,2 \pm 43.5$ HU. For the bilateral hip implant cohort, the HU results with MAR algorithm were the closest of HUref (HUref(MAR)= -37.1 HU ; HUref(CBCT)= -262.6 HU ; HUref(no MAR)= -409.5 HU). The noise in the image was reduced too in comparison with images without MAR reconstruction and CBCT (σ (MAR)= 104.9 HU ; σ (CBCT)=153.2 HU ; σ (no MAR)= 211 HU).

Conclusion: The reconstruction quality of soft tissues between a bilateral hip implant was improved with MAR algorithm by reducing artifacts, noise and by increasing the HU accuracy. Dosimetric impact remains to be assessed (= -409.5 HU). The noise in the image was reduced too in comparison with images without MAR reconstruction and CBCT (σ (MAR)= 104.9 HU ; σ (CBCT)=153.2 HU ; σ (no MAR)= 211 HU).

EP-1830

Comparison of the MRI sequences in ideal fiducial marker-based radiotherapy for prostate cancer

O. Tanaka¹, M. Hattori¹, S. Hirose¹, T. Iida¹, T. Watanabe¹

¹Gifu Municipal Hospital, Department of Radiation Oncology, Gifu, Japan

Purpose or Objective: Image guided radiotherapy for prostate cancer is a sophisticated treatment modality. However, the contouring the prostate is difficult to achieve with CT alone. To overcome the uncertainty of contouring the target on CT images, MRI is used in the registration of CT in addition to MRI using a fiducial marker. However, the visualization of the markers tends to be difficult in MRI. The aim of the present study is to find an optimal MRI pulse sequence for defining the marker as well as the prostate outline by comparing five different sequences.

Material and Methods: A total of 21 patients were enrolled in the present study. The two gold fiducial markers were placed on the prostate 3 weeks before the CT/MRI examination. MRI was performed using a five-channel sense cardiac coil. We obtained five T1-weighted spin-echo sequences (repetition time [TR]/echo time [TE] in milliseconds: 400/8) (T1WI), T2-